Journal of Applied Sciences

ISSN 1812-5654

ANSInet
an open access publisher
http://ansinet.com

Journal of Applied Sciences 6 (13): 2768-2773, 2006
ISSN 1812-5654

Optimization in Implant Topology to Reduce Stress Shielding Problem

[1]M.I.Z. Ridzwan, [1]Solehuddin Shuib, [1]A.Y. Hassan, [2]A.A. Shokri and [3]M.N.M. Ibrahim
[1]School of Mechanical Engineering, University of Science Malaysia,
14300 Nibong Tebal, Penang, Malaysia
[2]Department of Orthopaedic, School of Medical Sciences, Health Campus,
University of Science Malaysia, 16150 Kubang Kerian, Kelantan, Malaysia
[3]School of Chemical Sciences, University of Science Malaysia, 11800 Penang, Malaysia

Abstract: Introducing an implant into a femur might reduce the natural stress distribution of the femur. The reduction could cause its density and volume shrinkage. The implant starts to loose and causes patients hardly to move, thus needed a revision surgery. The phenomenon of reduction in load was identified as stress shielding. Topology optimization method was employed in the analysis of model of implant, cement and femur in 3-dimension by using ANSYS 7.1. The objective of the optimization was to minimize implant compliance subjected to percentage of reduction in its initial volume (V_0) ranges from 30% up to 70% V_0. Results showed that implant with 50 or 60% V_0 would produce closed boundary and hence were acceptable in shape. Both implants were compared in stress distribution with conventional implant and intact femur (without implant). Load transfer has increased in femur with the optimized implants compared to before optimize in medial and lateral side. Hence, it showed that the new optimized implants were better than the conventional implant in order to reduce stress shielding problem.

Key words: Stress shielding, topology optimization method, hip prosthesis, finite element analysis

INTRODUCTION

Hips are very important in helping us to accomplish our daily activities such as walking to the workplace, playing games, cycling, getting up from the seat, climbing upstairs etc. Unfortunately, there is no guarantee that our hips will always be in a good condition. Thigh bone or femur can be broken in an accident or damaged by osteoporosis and disease like rheumatoid arthritis. Damaged femur needs to be replaced with an implant through the operation like total hip arthroplasty or hemiarthroplasty.

Over 800,000 artificial hip joints have been implanted worldwide annually suggesting that it is a successful and well-accepted treatment (Li *et al*., 2003). However, patients still have possibility of suffering long-term side effect. Many implants are loosened within the femur after 10 years, which eventually leads to implant failure (Kuiper, 1993). Mechanical loosening of the implant is one of the most frequent complications after hip replacement which resulted from implant movement or migration in the bone or cement (Tang *et al*., 2002). Implant position may slightly change in comparison to its initial location resulting from loss of bone mass. This has been a result of stress shielding and occurs in cemented and cement less implants.

Based on the principle known as Wolff's Law, stress shielding refers to the tendency of bone to atrophy when it does not receive adequate mechanical loading. Originally, the bone carries its external load by itself. When implant is introduced into the femur, now the bone has to share the load and the carrying capacity with the implant. As a result, the bone is subjected to reduced stresses and hence stress shielded (Huiskes *et al*., 1992). Many studies have demonstrated that there would be a reduction in stress and relative density occurred in a proximal femur after arthroplasty. Stress reduction observed in implanted bone will lead to bone resorption and implant loosening. It can cause difficulties to patients, thus they might require a revision surgery.

Bone receives more loads if stem can be eliminated from the implant. Consequently, a stemless implant was designed. It was fixed with several screws (Munting and Verhelpen, 1995) or cables and square plate to support the head (Joshi *et al*., 2000). However, Munting and Verhelpen (1995) has claimed that the stemless implant

Corresponding Author: Solehuddin Shuib, School of Mechanical Engineering, University of Science Malaysia
Tel: 6045996324 Fax: 6045941025

was effective for short term fixation and besides there were no significant data or results proving that the problem can be reduced in real situation. In another study, hollow geometry has been introduced by increasing stem inner diameter to reduce stress shielding (Gross and Abel, 2001). However, the study only used a cylindrical shape with a simple point load and boundary conditions. Stress shielding can also be decreased if stem is made from non-stiff material which has modulus Young equal to bone (Morscher and Dick, 1983; Ridzwan *et al*., 2006). But, flexible implant may produce higher stresses along the interface (Huiskes *et al*., 1992).

This study is to obtain an optimum implant that can reduce the problem of stress shielding by using topology optimization method. The optimum implant will be compared to the reference implant.

MATERIALS AND METHODS

Topology optimization method solves optimization problem through distributing a given amount of material freely in a design space so that performance is optimized. The method combines Finite Element Method (FEM) and optimization algorithm (e.g., developing mathematical programming (Fujii and Kikuchi, 2000; Pedersen *et al*., 2001) or using built in optimization software (Kosaka *et al*., 2000; Thomas *et al*., 2002) to find the optimal material distribution in a fixed design domain. In relation to the main problem, implant design was taken as an example in each step in optimization. Figure 1 shows an overall flowchart of the methodology to achieve the main objective.

Design domain: A study was performed using a commercial Finite Element (FE) package, i.e., ANSYS 7.1. The model of implanted femur was shown in Fig. 2. The implant geometry was taken from Westfield Medical Ltd., while the bone which was similar to Sawbones cement pressure, was taken from Depuy International Ltd. The cement was filled up between the implant and the bone

Table 1: Material properties used in FE model

Parts	Elastic modulus, E (GPa)	Poisson's ratio, ν
Implant (Titanium)	115	0.3
Cement	2	0.3
Cortical bone	20	0.3

Table 2: Applied load cases with resultant maximum value

	Loads	F_x (N)	F_y (N)	F_z (N)
1	F_a	-768	-726	1210
	F_h	224	972	-2246
2	F_a	166	382	957
	F_h	136	-630	-1692
3	F_a	383	669	547
	F_h	457	-769	-1707

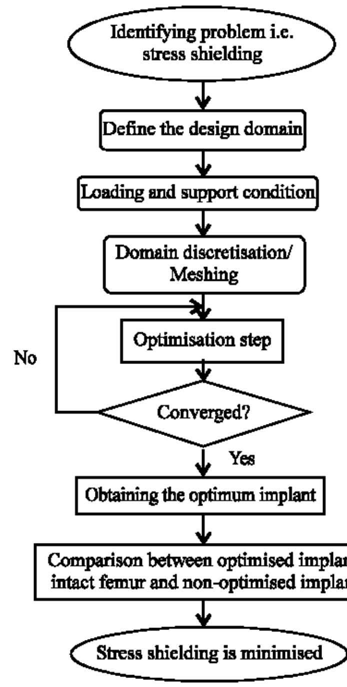

Fig. 1: Flowchart of methodology

and the gap was set to be 3 mm. The model was rotated in 12° from vertical axis as done by Lennon *et al.* (2003) and divided into three types, corresponding to three different materials. The implant was identified as type 1 was the only part that being optimized and the other two types were not. Properties of materials used for FE were shown in Table 1.

Discretisation/meshing: In FE model, implant-cement-bone interfaces were bonded. All materials were assumed linearly isotropic and homogeneous. The model used twenty nodes hexahedral finite element (ANSYS type SOLID95). The element length given to each material was varied. Implant should be meshed smoothly otherwise, it would result with coarser surface in the final topology. The model consisted of 12,201 numbers of elements with 7,287 elements for implant, 1,498 (cement) and 3,416 (bone).

Boundary conditions: The distal end of bone was rigidly fixed in the x, y and z directions, that are $U_x = 0$, $U_y = 0$ and $U_z = 0$. Loads were applied at the proximal end of stem (F_h) and abductor muscle (F_a) as shown in Fig. 3. The applied load case was similarly as described in Fernandes *et al.* (2002). However, for the optimization purposes, only one load case with the maximum resultant value was considered. It was corresponded to walking movement as shown in Table 2.

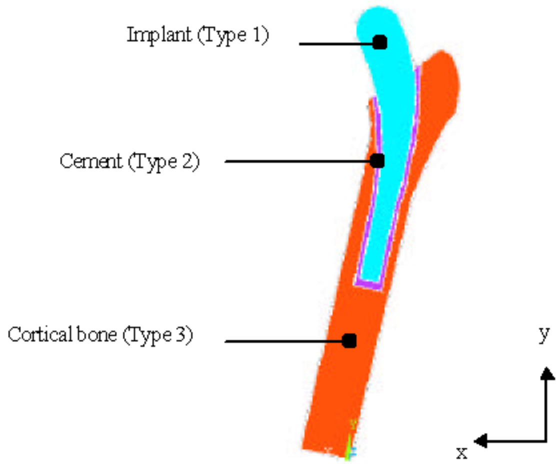

Fig. 2: Design domain

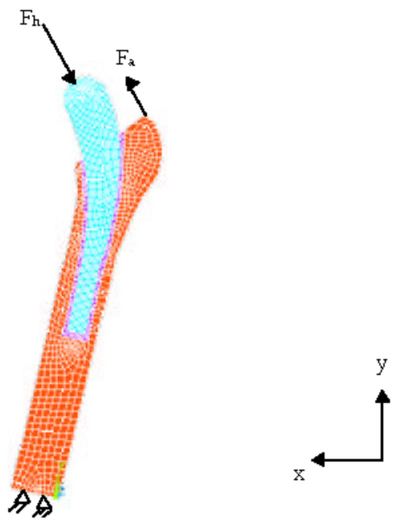

Fig. 3: Meshed domain and applied boundary conditions

Mathematical formulation: The theory of topology optimization seeks to minimize or maximize the objective function, f subject to the constraints defined. The design variables (ρ_i) are densities that are assigned to each finite element in the design domain. The density for each element varies from 0 to 1; where $\rho_i = 0$ represents material to be removed and $\rho_i = 1$ represents material that should be kept.

This study was to minimize the implant compliance subject to its volume reduction. Localized stress as optimization criteria probably is the best but this is not possible as the study looks into the distribution of the stress pattern. The next alternative is to use compliance as the objective function as has been used by Fernandes *et al*. (2002).

In this case, we applied six points of loads as shown in Table 2. Therefore, f would be stated as:

$$f(U_c^1, U_c^2, \ldots, U_c^6) = \sum_{i=1}^{6} W_i U_c^i,\ W_i \geq 0 \quad (1)$$

Subject to:

$$0 < \rho_i \leq 1 \qquad (i = 1, 2, 3, \ldots N) \quad (2)$$

$$V \leq V_o - V^* \quad (3)$$

Where:

W_i = Weight for load case with energy U_c
V = Computed volume
V_o = Original volume
V^* = Amount of materials to be removed

The reductions of volume were set to be 30, 40, 50, 60 and 70% from the initial implant volume, V_o.

RESULTS AND DISCUSSION

Topology results and design interpretation: The results for every % V_o were cut in z-direction in order to observe inside topology of the implants. Generally, every implant was cut into five sections with different thickness. Table 3 shows implant topologies for each material constraint case in the x-y plane in given z-direction. The topologies represented the value of relative density, ρ_i between 0.89-1, which supposedly solid.

Elements with high relative density values mean that they retain high Young's modulus and high stress values while low relative density elements are assigned low Young's modulus and low stressed elements values. Elements with high stress values mean that they were subjected to high loads and would be kept and remained meanwhile, elements with low stress values mean subjected to less loads and would be removed.

Every solution was topologically different. The main difference was seen at proximal end of implant, especially between thicknesses 1.85 to 10.90 mm. The solutions of 70, 40 and 30% V_o had developed an open boundary whereas 50 and 60% V_o had developed the closed boundary and produced acceptable shape. Therefore, these designs were chosen for shape refinement.

As mentioned earlier, the objective function was to minimize the implant compliant subjected to its required volume. Figure 4 shows a comparison in implant compliance at different volume reductions. The graphs were obtained from ANSYS 7.1 during iterations to get the optimum results. From the figure, a good relation was seen between number of iterations and acceptable implant topologies. More than 30 iterations were required in order to produce satisfactory topologies. Besides, it also showed that implant with the least volume, i.e., 30% V_o,

Table 3: Implant topologies about x-y plane in z-direction with different implant volumes

Percentages of volume, % V_0	Implants cross sections in z-direction (mm): 0.05	1.85	3.65	9.10	10.90	12.65
70	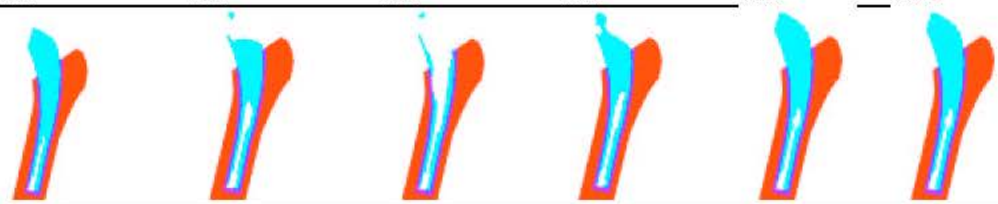					
60	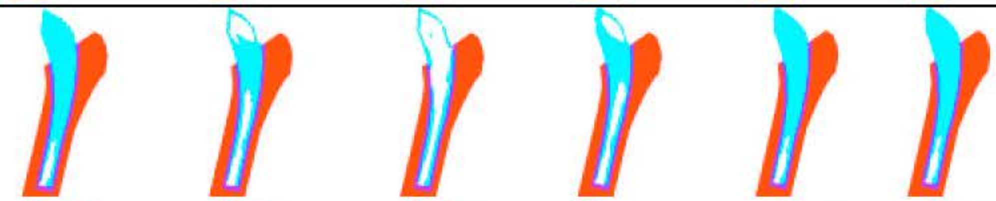					
50	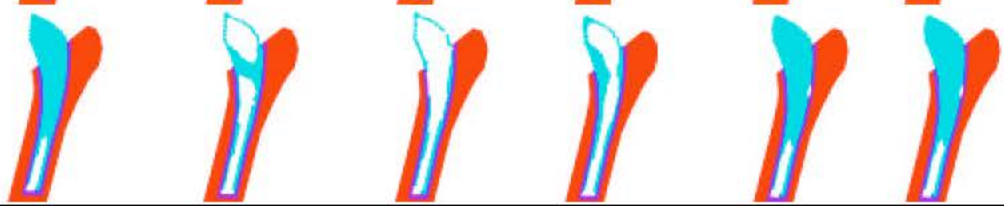					
40	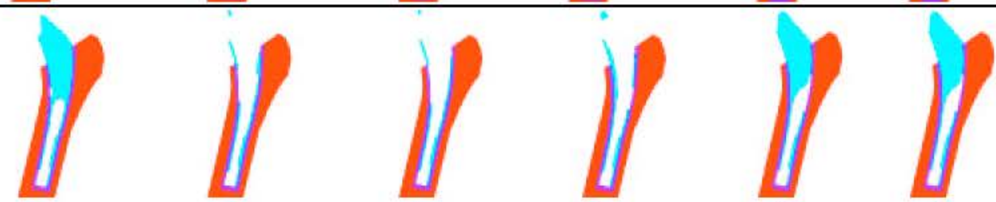					
30	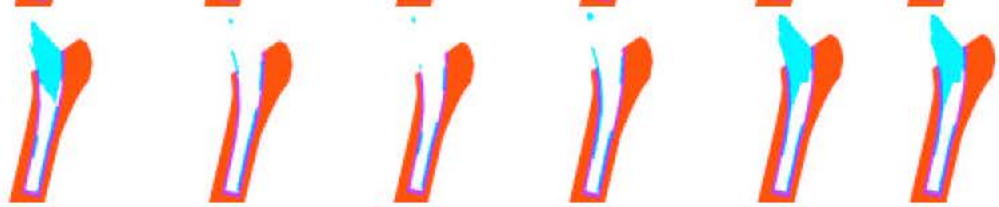					

was the most compliance. During the analysis, one single data that was produced in the Fig. 4 required almost one and a half hour of computational time.

Shape refinements: The topology optimization results as shown in Fig. 5a and b were extracted from Table 3. The figure presented five different topologies obtained from one of the optimum implants. It was difficult to interpret since they contain zigzag border. Excepting boundaries inside the implant were shown as the bold lines in Fig. 5b (Sun, 2004). Commercial CAD software, i.e., AutoCAD 2002 was used to refine the model.

Figure 6 showed the inside topology of the optimum implant in 3-dimension. Only half of its size was modelled to show its inside topology. The 3D implant was obtained after combined all sections that had been refined as in Fig. 5b. The implant maintained its external surface as

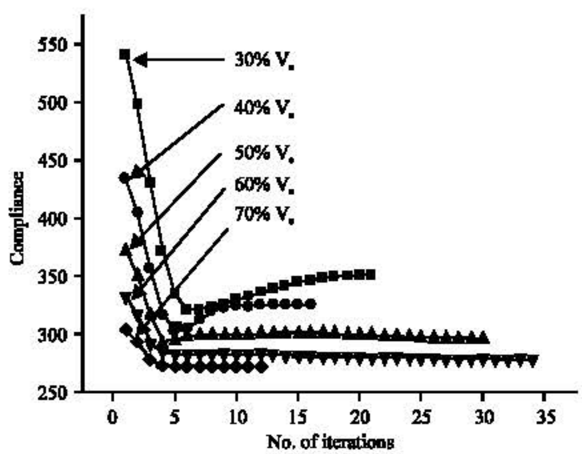

Fig. 4: Comparison in implant compliance at different volume reductions

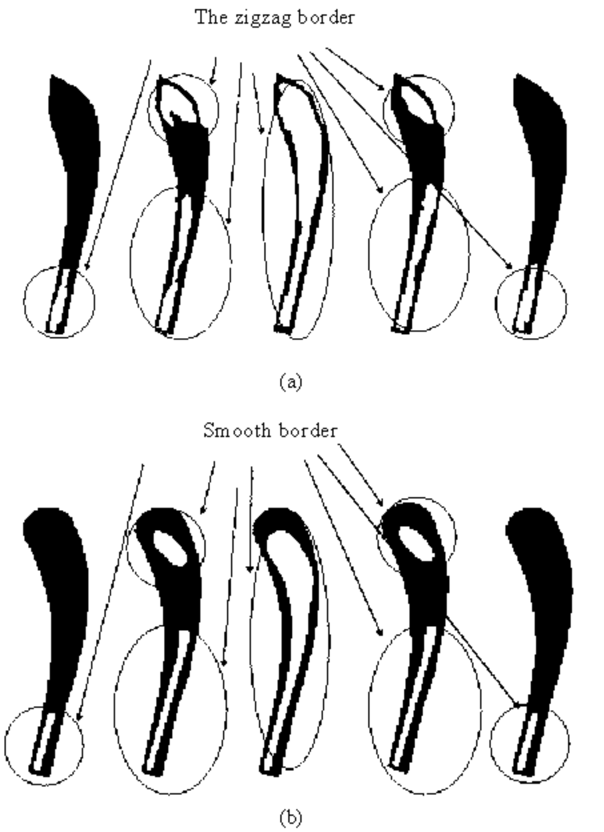

Fig. 5: Result of topology optimum design 60% V_o with (a) zigzag border and (b) after shape refinement.

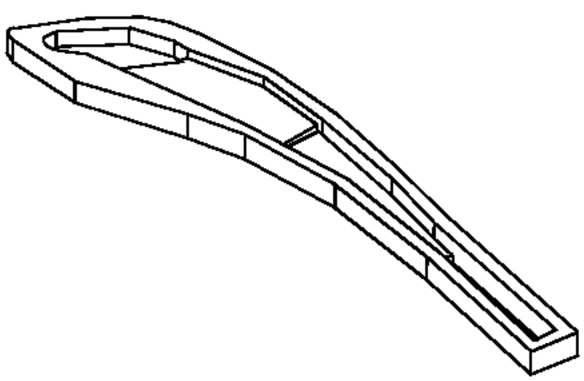

Fig. 6: A brief design according to the result of topology optimum method. Only half of its size was modelled to show its inside topology

before optimized. Topology optimization method had created the hole inside the implant and optimized the hole to achieve the required objective. The implant was no longer stiff as before being optimized and also not too compliance. Stiffer implant might create stress shielding to the bone and if it was too compliant, it might develop higher stress along the bone-implant interface.

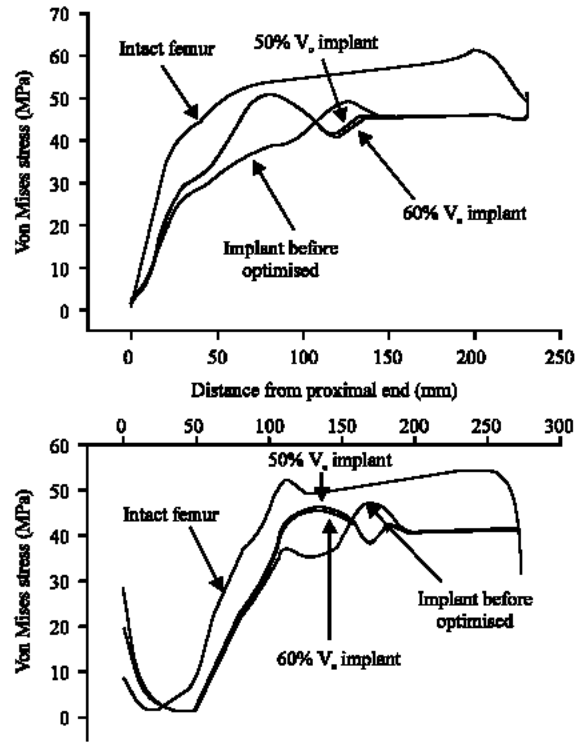

Fig. 7: Von Mises stresses of the femur along medial (top) and lateral (bottom) side

Comparison results: Stresses along medial and lateral side in intact and implanted femur were plotted and compared with optimum models. Loading and boundary conditions applied were similar as in Table 2.

The von Mises stresses in the femur, as shown in Fig. 7 had occurred along medial and lateral side. Stresses produced in both optimum models were very close to each other and were almost lie on the same line. This was caused by the approximately same topologies for both implants. In medial side, both implants increased the stress after one fifth of the femur.

In lateral side, tensile stress was very low in the beginning, but it started to increase after one third of the femur and was maintained until the end. This was probably because of the wide cross sectional area around the greater trochanter. The maximum stress occurred in the middle of the femur at the level of implant tip which meant that load transfer has increased in the femur with the optimized implants compared to before optimization.

Table 4 shows the maximum stresses and percentage of load distribution occur in femur along medial and lateral sides. The percentages were obtained by using a formula below:

$$\% \text{ Area} = \frac{A_o - A_f}{A_o} \times 100\% \quad (4)$$

Table 4: Load distribution occurs in femur

Models	Percentage of decrease in load distribution at medial side (%) A_o = 11738.26 mm^2	Percentage of decrease in load distribution at lateral side (%). A_o = 10631.90 mm^2
Intact femur	N/A	N/A
Implant before optimized	24.75	23.72
60% V_o implant	20.94	20.54
50% V_o implant	20.72	20.95

Where:

A_o = Area below graph for intact femur

A_f = Area below graph for other models

From Table 4, we could observe that both optimum implants have shown increments in load distribution to the femur in comparison to the conventional implant. Although the differences between optimum and conventional implants were not too marginal, but, it has been proven in Fig. 7 that the optimized implants have tried to bring the stress as closed as in intact femur especially along the length of implants. Hence, it showed that the new optimized implants were better than conventional implant in order to reduce stress shielding problem.

CONCLUSIONS

The phenomena of stress shielding occurred after the implant was inserted into the femur. The problem came when the metal implant took more loads which originally transferred only to the femur. For the past few years, many methods to reduce the problem have been applied by several of researchers.

In this study, topology optimization method was applied in the design of implant to reduce the problem known as stress shielding. The method generates and simultaneously optimizes the holes in the stem. This application confirmed that the femur in optimized implant receives more load compared to the femur in the implant without optimized.

ACKNOWLEDGEMENT

This study is supported b a short term USM IRPA under grant No. 6035120.

REFERENCES

Fernandes, P.R., J. Folgado, C. Jacobs and V. Pellegrini, 2002. A contact model with ingrowth control for bone remodeling around cement less stems. J. Biomechanics., 35: 167-176.

Fujii, D. and N. Kikuchi, 2000. Improvement of numerical instabilities in topology optimization using the SLP method. Structural Multidisciplinary Optimization, 19: 113-121.

Gross, S. and E.W. Abel, 2001. A finite element analysis of hollow stemmed hip prostheses as a means of reducing stress shielding of the femur. J. Biomechanics, 34: 995-1003.

Huiskes, H.W.J., H. Weinans and B. van Rietbergen, 1992. The relationship between stress shielding and bone resorption around total hip stems and the effects of flexible materials. Clin. Orthopaedics, 274: 124-134.

Joshi, M.G., S.G. Advani, F. Miller and M.H. Santare, 2000. Analysis of a femoral hip prosthesis designed to reduce stress shielding. J. Biomechanics, 33: 1655-1662.

Kosaka, I., C. Charpentier and B.C. Watson, 2000. An interface between SDRC I-DEAS and the GENESIS structural analysis and optimization code. Proceedings in the AIAA-2000-493, American Institute of Aeronautics and Astronautics.

Kuiper, J.H., 1993. Numerical optimization of artificial hip joint designs. Ph.D Thesis. Katholieke Universiteit Nijmegen.

Lennon, A.B., B.A.O. McCormack and P.J. Prendergast, 2003. The relationship between cement fatigue damage and implant surface finish in proximal femoral prostheses. Med. Eng. Phys., 25: 833-841.

Li, C., C. Granger, H.D. Schutte, S.B. Biggers, J.M. Kennedy and R.A. Latour, 2003. Failure analysis of composite femoral components for hip arthroplasty. J. Rehabil. Res. Develop., 40: 131-146.

Morscher, E.W. and W. Dick, 1983. Cement less fixation of isoelastic hip endoprostheses manufactured from plastic materials. Clin. Orthopaedics, 176: 77-87.

Munting, E. and M. Verhelpen, 1995. Fixation and effect on bone strain pattern of a stemless hip prosthesis. J. Biomechanics, 28: 949-961.

Pedersen, C.B.W., T. Buhl and O. Sigmund, 2001. Topology synthesis of large-displacement compliant mechanisms. Intl. J. Num. Meth. Eng., 50: 2683-2705.

Ridzwan, M.I.Z., S. Shuib, A.Y. Hassan and A.A. Shokri, 2006. Effects of increasing load transferred in femur to the bone-implant interface. J. Applied Sci., 6: 183-189.

Sun, S.H., 2004. Optimum topology design for the stationary platen of a plastic injection machine. Computers in Industries, 55: 147-158.

Tang, H., Y. Jiang, X.Z. Luo, S.M. Ren and H.K. Genant, 2002. Assessment of periprosthetic bone loss after total hip arthroplasty. Chine Med. J., 115: 510-513.

Thomas, H., M. Zhou and U. Schramm, 2002. Issues of commercial optimization software development. Structural and Multidisciplinary Optimization, 23: 97-110.